Journal of proteome research

Article

pubs.acs.org/jpr

Human Metabolic Responses to Chronic Environmental Polycyclic Aromatic Hydrocarbon Exposure by a Metabolomic Approach

Zhonghua Wang,[†] Yajie Zheng,[†] Baoxin Zhao,[‡] Yanping Zhang,[‡] Zhe Liu,[§] Jing Xu,[†] Yanhua Chen,[†] Zhao Yang,[∥] Fenfen Wang,[∥] Huiqing Wang,[†] Jiuming He,[†] Ruiping Zhang,*[,†] and Zeper Abliz*[,†]

[†]State Key Laboratory of Bioactive Substance and Function of Natural Medicines, Institute of Materia Medica, Chinese Academy of Medical Sciences and Peking Union Medical College, 1 Xiannongtan Street, Beijing 100050, China

[‡]Taiyuan Centre for Disease Control and Prevention, Taiyuan 030012, China

[§]Department of Biostatistics, Harvard School of Public Health, Harvard University, Boston, Massachusetts 02115, United States

[∥]School of Public Health, Shanxi Medical University, Taiyuan 030001, China

S *Supporting Information*

ABSTRACT: The toxicities of polycyclic aromatic hydrocarbons (PAHs) have been extensively explored due to their carcinogenic and mutagenic potency; however, little is known about the metabolic responses to chronic environmental PAH exposure among the general population. In the present study, 566 healthy volunteers were dichotomized into exposed and control groups to investigate PAH-induced perturbations in the metabolic profiles. Nine urine PAH metabolites were measured by a sensitive LC−MS/MS method to comprehensively evaluate the PAH exposure level of each individual, and the metabolic profiles were characterized via a LC−MS-based metabolomic approach. PAH exposure was correlated to its metabolic outcomes by linear and logistic regression analyses. Metabolites related to amino acid, purine, lipid, and glucuronic acid metabolism were significantly changed in the exposed group. 1-Hydroxyphenanthrene and dodecadienyl-carnitine have potential as sensitive and reliable biomarkers for PAH exposure and its metabolic outcomes, respectively, in the general population. These findings generally support the hypothesis that environmental PAH exposure causes oxidative stress-related effects in humans. The current study provides new insight into the early molecular events induced by PAH exposure in the actual environment.

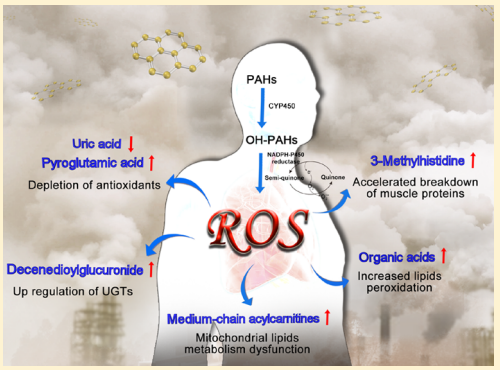

KEYWORDS: *Metabolomics, PAH exposure, oxidative stress, environmental health, molecular epidemiology*

INTRODUCTION

Environmental pollution, especially air pollution, is a worldwide problem and is particularly serious in developing countries. Polycyclic aromatic hydrocarbons (PAHs) are ubiquitous environmental pollutants that are produced by incomplete combustion of organic materials and are the predominant contaminants of coke oven emissions due to the incomplete combustion of coal. The health effects of PAH exposure have been widely studied, mainly because they are potentially carcinogenic and mutagenic. Reportedly, the association of air pollution with an increased risk of cancers and cardiopulmonary diseases is mainly due to PAH exposure.[1−3] Recent studies have indicated that children and elderly people are especially vulnerable to environmental toxicants, including PAHs.[4−7]

Human biomonitoring provides an integrated assessment of toxicant exposure through various routes, such as inhalation, ingestion, and dermal uptake, and takes into account the variations in pharmacokinetic processes (including absorption, distribution, metabolism, and elimination), which are particularly valuable for the evaluation of personal exposure to multiple forms of environmental contaminants such as PAHs.[8,9] Urinary 1-hydroxypyrene (1-OHP) has been widely used as a biomarker to monitor recent exposure to PAHs. However, the composition of PAH mixtures may vary among sources, meaning that urinary 1-OHP alone cannot reflect the overall PAH exposure.[10] In addition, 1-OHP is thought to mimic the absorption of particle-bound PAHs through the lungs and skin, whereas monohydroxynaphthalenes and monohydroxyphenanthrenes are more specific markers of PAH inhalation.[11] Thus, multiple PAH metabolites need to be measured to obtain more accurate information about total PAH exposure in humans.

Understanding the early molecular events in the exposure−disease continuum will provide valuable information that can be used to intervene and change the outcome. Metabolomics is a promising molecular profiling technology that can detect the biological consequences of toxicant exposure by identifying metabolic biomarkers that correlate with exposure and predict health end points, termed a meet-in-the-middle strategy.[12,13] Such markers would help to elucidate the mechanism

Received: February 12, 2015
Published: May 20, 2015

DOI: 10.1021/acs.jproteome.5b00134
J. Proteome Res. 2015, 14, 2583−2593

underlying the toxicity and disease etiology in the human population and could ultimately inform follow-up monitoring of populations subjected to environmental pollution.[14] In addition, in comparison to targeted toxicological methods, global metabolomics does not focus on any specific analyte. Rather, it provides a high-throughput and unbiased evaluation of the metabolic responses of organisms to toxic stimuli, which makes it especially useful when the compositions of the toxicants are complicated and unknown.[15] Metabolomics has been used to investigate the health effects of human environmental exposure to several environmental pollutants, such as cadmium, arsenic, and welding fumes.[14,16−18] However, to our knowledge, little is known about the human metabolic response to chronic environmental PAH exposure.

In this study, a LC−MS-based metabolomic approach was used in conjunction with multivariate statistical data analyses to investigate the perturbations in human systemic metabolism. This was achieved by analyzing the urine samples of a large population of children and elderly people living in an area polluted by the coking industry and a nonpolluted control area. Metabolic alterations in response to PAH exposure were evaluated to discover potential metabolic biomarkers. In addition, the level of PAH exposure in the same population was evaluated by measuring nine urinary PAH metabolites using a sensitive LC−MS/MS method. Finally, correlation analyses between personal PAH exposure and its metabolic consequences were performed to evaluate the dose−effect relationship. The research strategy is shown in Figure 1.

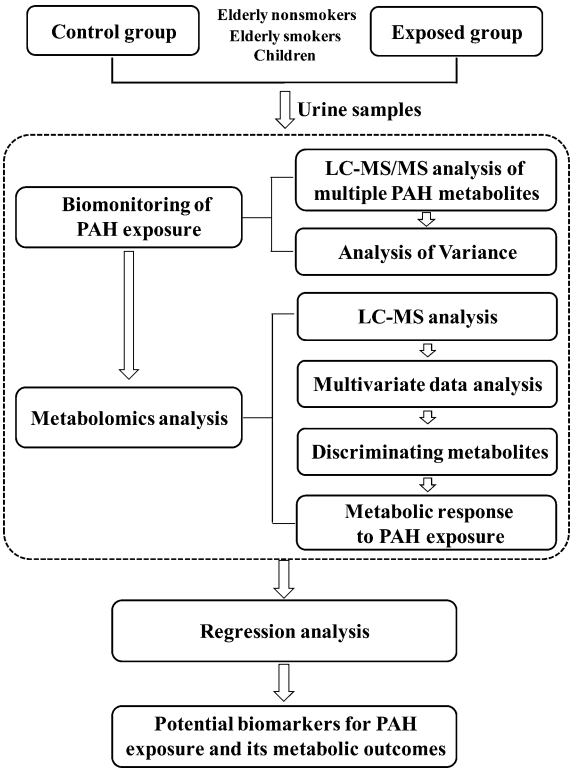

Figure 1. Research scheme for chronic exposure to environmental PAHs among the general population by an LC−MS-based metabolomic approach.

MATERIALS AND METHODS

Chemicals

HPLC-grade acetonitrile, methanol, and formic acid were purchased from Merck (Darmstadt, Germany). 1-Hydroxynaphthalene (1-OHN), 2-hydroxynaphthalene (2-OHN), 1-hydroxyphenanthrene (1-OHPH), 2-hydroxyphenanthrene (2-OHPH), 3-hydroxyphenanthrene (3-OHPH), and 4-hydroxyphenanthrene (4-OHPH) were purchased from Dr. Ehrenstorfer (Augsburg, Germany). 2-Hydroxyfluorene (2-OHF) was purchased from Sigma-Aldrich (Munich, Germany). 1-OHP and 6-hydroxychrysene (6-OHC) were purchased from AccuStandard (New Haven, CT). The internal standards, [$^{13}C_6$]3-hydroxyphenanthrene ([$^{13}C_6$]3-OHPH) and [$^{13}C_6$]6-hydroxychrysene ([$^{13}C_6$]6-OHC), were purchased from Cambridge Isotope Laboratories, Inc. (Andover, MA, USA). All standard samples used in metabolomic analysis, including L-carnitine, hexanoylcarnitine, phenylalanine, tryptophan, leucine, tyrosine, adenine, uridine, linoleic acid, cholic acid, kynurenic acid, progesterone, 3-methyl-L-histidine, L-pyroglutamic acid, uric acid, 2-isopropylmalic acid, and azelaic acid, were purchased from Sigma-Aldrich (St. Louis, MO, USA).

Study Subjects

Two-hundred thirty-eight elderly nonsmokers, 114 elderly smokers, and 214 children were included and dichotomized into the exposed and control groups. The general characteristics of the participants are summarized in Table 1. The participants in the exposed groups were from a polluted rural area less than 2 km downwind of a large coking plant, whereas the individuals in the control groups were from a nonpolluted national ecological demonstration area. The two areas are located in the south of Shanxi province, China, are approximately 70 km apart, and share similar climate conditions, socioeconomic status, population composition, and pattern of life. The total concentrations of the United States Environmental Protection Agency (US EPA) 16 priority PAHs in ambient air, dustfall, soil, and food in the polluted area were 65, 15, 6, and 2.2 times higher than those in the nonpolluted area (Taiyuan CDC, unpublished data). A self-administered questionnaire was used to collect information about the participants' medical, cardiopulmonary, smoking, drinking, and occupational histories. Individuals with a history of cardiopulmonary and/or chronic inflammatory diseases were excluded from the study. Written informed consent was obtained from each participant. Fasting spot urine samples

Table 1. General Characteristics of the Participants in the Control and Exposed Groups

characteristic	category	control group	exposed group
no. of subjects	elderly nonsmokers	96	142
	elderly smokers	35	79
	children	66	148
male/female	elderly nonsmokers	28/68	52/90
	elderly smokers	35/0	79/0
	children	32/34	84/64
age (years) (mean ± SD)	elderly nonsmokers	58.8 ± 8.6	61.9 ± 7.6
	elderly smokers	59.7 ± 6.9	59.1 ± 7.0
	children	7.2 ± 1.4	7.0 ± 1.4

DOI: 10.1021/acs.jproteome.5b00134
J. Proteome Res. 2015, 14, 2583−2593

were collected from all subjects before breakfast and were stored at −80 °C until analysis. All samples were collected in the summer.

Measurement of Urinary PAH Metabolites

The concentrations of nine urinary PAH metabolites, namely, 1-OHN, 2-OHN, 2-OHF, 1-OHPH, 2-OHPH, 3-OHPH, 4-OHPH, 1-OHP, and 6-OHC, were determined using a previously described LC−MS/MS method with some modifications.[19] Briefly, after adding 50 μL of the internal standards ([$^{13}C_6$]3-OHP and [$^{13}C_6$]6-OHC, 50 ng/mL), 10 mL of the urine sample was acidified and buffered with 0.2 N hydrochloric acid/0.5 M acetate buffer (pH 5) and hydrolyzed by β-glucosidase/aryl sulfatase (Sigma-Aldrich, Munich, Germany) at 37 °C for 12 h. The enzymatically hydrolyzed sample was cleaned up on a Bond Elut C_{18} cartridge (500 mg, 3 mL; Agilent Technologies, Loveland, CO, USA) and eluted with 5 mL of acetonitrile (containing 0.05% ammonia). The eluent was further dried in a centrifugal vacuum concentrator (SPD121P, Thermo Scientific, Germany) at 50 °C and reconstituted in 500 μL of 50% methanol. Finally, 10 μL of the extracts was analyzed using a rapid resolution LC system (Agilent Technologies, Waldbronn, Germany) coupled to a QTRAP 5500 mass spectrometer (AB SCIEX, Foster City, CA, USA) in negative ion and multiple reaction monitoring (MRM) modes using an Agilent ZORBAX SB-C_{18} column (150 × 3.0 mm i.d., 1.8 μm; Agilent Technologies, Santa Clara, CA, USA). More detailed information regarding the LC and MS conditions is available in Supporting Information Table S1 and S2.

All of the methods have been validated for linearity, sensitivity, precision, and accuracy. The lower limit of quantification (LLOQ) was defined as the lowest concentration analyzed with accuracy and precision within ±20%. Urine samples spiked with standard compounds were used as quality control (QC) samples and were analyzed via the same process to guarantee the quality of the data. The accuracy and precision for the QC samples had to be within ±15%. The concentrations of the nine metabolites were calculated from the standard curve generated in the same batch. The urinary creatinine concentration was analyzed using an enzymatic procedure.

Metabolomics Analysis

Sample Preparation. Frozen urine samples were allowed to thaw at 4 °C, vortexed, and centrifuged at 10 000*g* for 10 min at 4 °C. The supernatant was transferred to an Eppendorf tube, diluted with water so that the creatinine concentration was 625 μM and the volume was 800 μL, and centrifuged at 10 000*g* for 10 min at 4 °C. The supernatant was transferred to a new tube, and 10 μL was injected into the UHPLC−MS/MS system.

UHPLC−MS Analysis. Chromatographic separation was performed on a Zorbax Aq-C_{18} analytical column (1.8 μm, 10 cm × 2.1 mm; Agilent Technologies, Santa Clara, CA, USA) using a Shimadzu LC-30A Series UHPLC system (Shimadzu, Duisburg, Germany). The column was maintained at 50 °C and flushed with 0.1% formic acid−water (solvent A) and acetonitrile (solvent B) at a flow rate of 300 μL/min. The gradient conditions were as follows: 0−2 min, 0% solvent B; 2−13 min, linear gradient of 0−50% solvent B; 13−16 min, linear gradient of 50−100% solvent B; and 16−20 min, 100% solvent B.

MS was performed on a TripleTOF 5600 system (AB SCIEX, Foster City, CA, USA) using a duo spray source with a separate electrospray ion (ESI) source and an atmospheric pressure chemical ionization (APCI) source. The ESI source was used for urinary metabolomic profiling, whereas the APCI source was used as the second gas heater and for exact mass calibration of the QqTOFMS instrument. Data were acquired in both positive and negative ion modes. The instrumental conditions were as follows: ESI, source voltage 5.5/−4.5 kV; vaporizer temperature, 450 °C; turbo gas, 50 psi; nebulizer gas, 60 psi; curtain gas, 35 psi; and declustering potential, 50/−50 V. The scan range was m/z 50−800. Nitrogen gas was used for both nebulizing and drying. The data were acquired and processed using Analyst TF (version 1.6, AB SCIEX).

In the MS/MS experiments, the TripleTOF 5600 system was operated using an information-dependent acquisition method to collect full-scan MS and MS/MS information simultaneously. The signals were detected in a TOF survey scan, and the eight most intense parent ions were selected for MS/MS fragmentation spectra acquisition. The metabolites of interest were included in the MS/MS table list. The collision voltage was linearly ramped from 20 to 50 V or from −20 to −50 V. Exact mass calibration was performed automatically before each analysis using the Automated Calibration Delivery System (AB SCIEX).

Pooled urine samples were processed as QC samples and randomly placed in the sample queue to monitor the stability of the LC−MS system.[20] The samples from all participants were arranged in random order in the analysis batch. A test mixture of the standard compounds, including L-carnitine, hexanoylcarnitine, phenylalanine, tryptophan, leucine, tyrosine, adenine, uridine, linoleic acid, cholic acid, kynurenic acid, and progesterone, was also analyzed at the beginning, middle, and end of the batch to visually evaluate the chromatographic reproducibility. The criteria used to assess the stability of the LC−MS system were as follows: the peak area deviations obtained by PCA analysis should be <2 SD for all QC samples and the within-batch retention time shifts and the peak area deviation of the standard compounds should not exceed 20 s and 20%, respectively.

Raw Data Processing. UHPLC−MS raw data files were converted to the mzXML format using the ProteoWizard msconvert tool (http://proteowizard.sourceforge.net/). Peak finding, filtering, alignment, and scaling were subsequently performed using open-source XCMS software (http://masspec.scripps.edu/xcms/xcms.php) operated within the R statistical software (version 2.15.2). The parameters for the detailed data preprocessing are available in the Supporting Information.

Statistical Analysis

The distribution of the numerical data was tested by the one-sample Kolmogorov−Smirnov normality test. Normal distributions of the urinary PAH metabolites were obtained by natural logarithmic (log) transformation. The Pearson correlation coefficients between the nine log-transformed PAH metabolites were calculated by a simple linear correlation analysis. Multivariate analysis of the processed metabolomics data obtained by UHPLC−MS analysis, including principal component analysis and orthogonal partial least-squares discriminant analysis (OPLS-DA), were performed with SIMCA-P software +12.0 (Umetrics AB, Umeå, Sweden). Analysis of variance (ANOVA) was used to compare the differences in the numerical variables. The dose−response relationships of PAH exposure with the metabolic outcomes were evaluated by logistic regression and linear regression

DOI: 10.1021/acs.jproteome.5b00134
J. Proteome Res. 2015, 14, 2583−2593

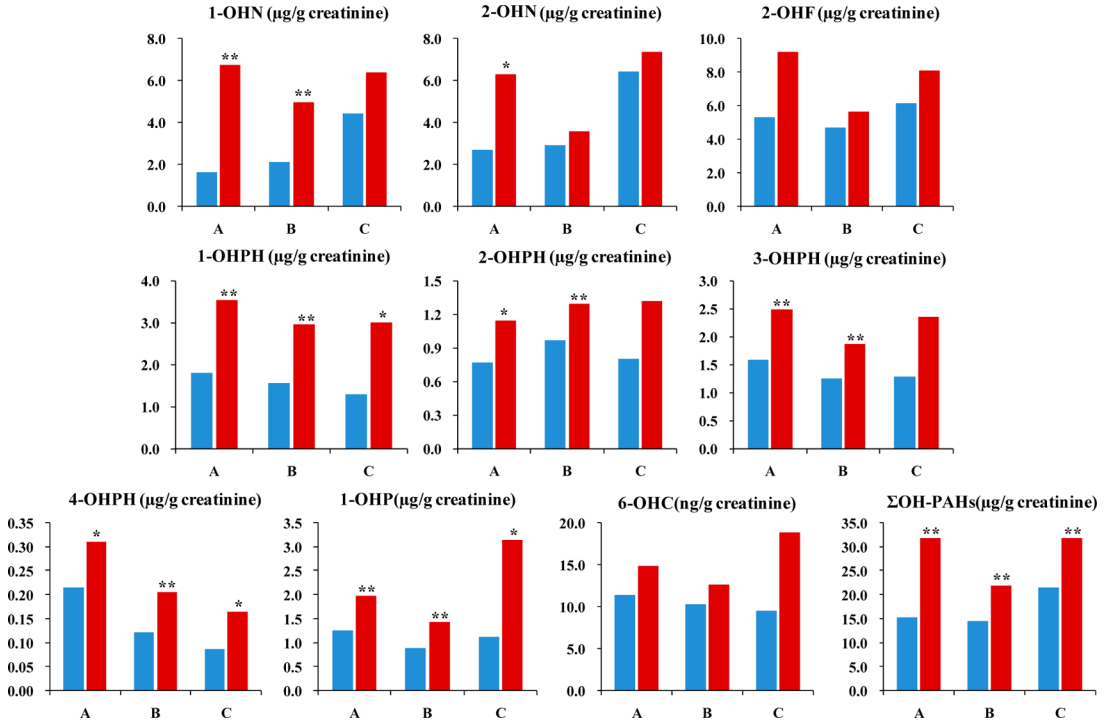

Figure 2. Mean levels of urinary PAH metabolites in the control and exposed groups (A, children; B, elderly nonsmokers; C: elderly smokers; blue bars, control group; red bars, exposed group). *, $p < 0.05$; **, $p < 0.01$.

analyses. All statistical analyses were performed in the R statistical systems, with the exception of multivariate analysis.

RESULTS

Profiles of the Urinary PAH Metabolites

We successfully detected nine urinary PAH metabolites. The LLOQ for the urinary PAH metabolites ranged from 3.75 to 15 pg/mL. Eight PAH metabolites (all except 6-OHC) were present above the LLOQ in more than 95% of the samples. 6-OHC was present above the LLOQ in 61% of samples in the exposed group and in 46% of samples in the control group. 2-OHF was the most abundant PAH metabolite, followed by 2-OHN and 1-OHN, and the concentration of 6-OHC was the lowest.

The concentrations of the nine urinary PAH metabolites and the sum of the concentrations of all nine PAH metabolites (∑OH-PAHs) are shown in Figure 2 and Supporting Information Table S3 (data adjusted for urinary creatinine). For elderly nonsmokers, the urinary concentrations of 1-OHN, 2-OHN, 2-OHF, 1-OHPH, 2-OHPH, 3-OHPH, 4-OHPH, 1-OHP, 6-OHC, and ∑OH-PAHs were 2.4, 1.2, 1.2, 1.9, 1.3, 1.5, 1.7, 1.6, 1.2, and 1.5 times higher in the exposed group than those in the control group, respectively. For children, the levels of 1-OHN, 2-OHN, 2-OHF, 1-OHPH, 2-OHPH, 3-OHPH, 4-OHPH, 1-OHP, 6-OHC, and ∑OH-PAHs were 4.2, 2.4, 1.8, 2.0, 1.5, 1.6, 1.5, 1.6, 1.3, and 2.1 times higher in the exposed group than those in the control group, respectively. For elderly smokers, the urinary concentrations of 1-OHN, 2-OHN, 2-OHF, 1-OHPH, 2-OHPH, 3-OHPH, 4-OHPH, 1-OHP, 6-OHC, and ∑OH-PAHs were 1.5, 1.2, 1.3, 2.3, 1.7, 1.8, 1.9, 2.8, 2.0, and 1.5 times higher in the exposed group than those in the control group, respectively.

The levels of the urinary PAH metabolites were also examined with respect to smoking status for the elderly male participants (Supporting Information Table S4). Among the control group, the urinary concentrations of 1-OHN, 2-OHN, 2-OHF, 1-OHPH, 2-OHPH, 3-OHPH, 4-OHPH, 1-OHP, 6-OHC, and ∑OH-PAHs were 2.6, 2.3, 1.5, 0.88, 0.78, 0.91, 0.80, 1.0, 1.4, and 1.6 times higher in smokers than those in nonsmokers, respectively. Among the exposed group, the urinary concentrations of 1-OHN, 2-OHN, 2-OHF, 1-OHPH, 2-OHPH, 3-OHPH, 4-OHPH, 1-OHP, 6-OHC, and ∑OH-PAHs were 1.8, 2.6, 1.4, 1.1, 0.94, 1.1, 1.1, 2.2, 1.8, and 1.6 times higher in smokers than those in nonsmokers, respectively. These results are consistent with previous reports that smoking can contribute to urinary 1-OHN, 2-OHN, 2-OHF, 1-OHP, and 6-OHC levels in nonoccupationally PAH-exposed populations,[21−23] indicating that smoking is an important confound that should be considered when assessing environmental PAH exposure.

The linear correlations between various PAH metabolites were investigated separately for the different populations. The Pearson correlation coefficients between PAH metabolites are shown in Supporting Information Table S5. The majority of the log-transformed concentrations of urinary PAH metabolites were significantly correlated with each other, with the exceptions of 2-OHN and 6-OHC among children and elderly nonsmokers in the exposed group ($p < 0.05$). The correlations between PAH metabolites were less significant in smokers, which may be due to the confounding factor of cigarette smoking.

Changes in the Urinary Metabolic Profiles with Different Levels of PAH Exposure

To investigate the global metabolome differences between the exposed and control groups, multivariate statistical analyses of the UHPLC−MS data were initially performed in elderly nonsmokers to avoid the potential confound of cigarette smoking. Supporting Information Figure S1 shows typical total

DOI: 10.1021/acs.jproteome.5b00134
J. Proteome Res. 2015, 14, 2583−2593

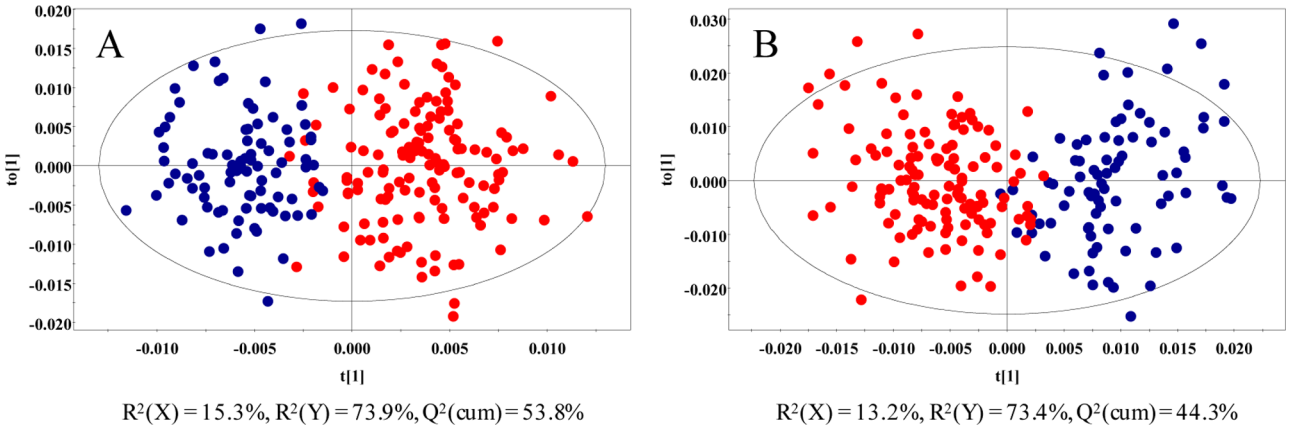

Figure 3. OPLS-DA score plots based on the (A) UHPLC−(+)ESI−MS and (B) UHPLC−(−)ESI−MS data from elderly nonsmokers. Blue dots, elderly nonsmokers in the control group (n = 96); red dots, elderly nonsmokers in the exposed group (n = 142).

Table 2. Metabolites Tentatively Identified That Are Capable of Discriminating between Elderly Nonsmokers in the Exposed and Control Groups

no.	RT[a]	m/z	elemental composition	metabolite identification	MS/MS data[d]	p value[e]	VIP[f]
1	0.87	170.0926	$C_7H_{12}N_3O_2$	3-Methylhistidine[b,c]	153, 135, 109, 95, 83, 68	3.45×10^{-3}	2.0
2	1.65	130.0496	$C_5H_8NO_3$	Pyroglutamic acid[b,c]	102, 84, 56, 41	7.12×10^{-5}	2.4
3	*2.07*	167.0213	$C_5H_3N_4O_3$	Uric acid[b,c]	124, 96, 69, 42	2.39×10^{-2}	5.7
4	5.68	302.1600	$C_{14}H_{24}NO_6$	Heptenedioylcarnitine[c]	243, 225, 197, 85, 60	4.58×10^{-4}	2.9
5	*5.9*	175.0614	$C_7H_{11}O_5$	2-Isopropylmalic acid[b,c]	157, 131, 115, 85, 59	1.13×10^{-2}	1.5
6	6.28	316.1764	$C_{15}H_{26}NO_6$	Octenedioylcarnitine[c]	257, 239, 211, 155, 85, 60	2.02×10^{-9}	3.9
7	6.98	330.1916	$C_{16}H_{28}NO_6$	Nonenedioylcarnitine[c]	271, 253, 225, 169, 85, 60	4.47×10^{-4}	2.4
8	*8.50*	375.1296	$C_{16}H_{23}O_{10}$	Decenedioylglucuronide[c]	199, 181, 175, 71, 57	1.82×10^{-3}	1.1
9	8.75	332.2422	$C_{17}H_{34}NO_5$	3-Hydroxydecanoylcarnitine[c]	255, 171, 153, 85, 60	6.48×10^{-3}	1.1
10	8.88	374.2535	$C_{19}H_{36}NO_6$	Dodecanedioylcarnitine[c]	315, 297, 171, 85, 60	5.58×10^{-4}	1.4
11	*9.38*	187.0976	$C_9H_{15}O_4$	Azelaic acid[b,c]	169, 143, 125, 97, 57	1.39×10^{-3}	2.6
12	*9.77*	199.0978	$C_{10}H_{15}O_4$	Decenedioic acid[c]	181, 155, 137, 99, 71	4.04×10^{-2}	1.2
13	10.2	302.2325	$C_{16}H_{32}NO_4$	Nonanoylcarnitine[c]	243, 159, 141, 85, 60	2.32×10^{-3}	4.3
14	*10.3*	273.1708	$C_{14}H_{25}O_5$	Hydroxytetradecanedioic acid[c]	255, 237, 175, 139, 59	1.28×10^{-2}	1.0
15	10.6	312.2171	$C_{17}H_{30}NO_4$	Decadienylcarnitine[c]	253, 169, 151, 85, 60	1.26×10^{-4}	1.3
16	11.0	358.2585	$C_{19}H_{36}NO_5$	Hydroxydodecenoylcarnitine[c]	299, 281, 155, 85, 60	2.32×10^{-3}	4.6
17	11.7	340.2482	$C_{19}H_{34}NO_4$	Dodecadienylcarnitine[c]	281, 197, 179, 85, 60	1.64×10^{-7}	13
18	12.2	342.2633	$C_{19}H_{36}NO_4$	Dodecenoylcarnitine[c]	283, 199, 181, 85, 60	3.18×10^{-5}	2.6

[a]RT values in italics and nonitalics are potential metabolic biomarkers that were detected in positive and negative electrospray ion modes, respectively. [b]Metabolites confirmed by standard compounds. [c]Metabolites provisionally identified by database searches and MS fragmentation. [d]MS/MS data were obtained with a CE of 20 to 50 eV or CE −50 to −20 eV, respectively. [e]p values calculated by independent Student's t test. [f]VIP is the variable importance in the projection obtained from OPLS-DA, with a threshold of 1.0.

ion chromatograms obtained from the urine samples of the different groups by UHPLC−MS analysis by ESI in positive ion mode (UHPLC−(+)ESI−MS). The data quality assessment (Supporting Information Figures S2 and S3) indicated that the significant differences observed between the groups by multivariate statistical analysis were likely due to genuine subtle changes in the metabolites rather than being products of artifacts arising from analytical errors. Using an optimized spectral data analysis protocol, 1400 and 637 features were extracted from the UHPLC−MS analysis by ESI in positive and negative ion modes (UHPLC−(±)ESI−MS), respectively. The metabolomic profiles of the two groups were compared by supervised multivariate OPLS-DA to achieve the maximum separation.[24] The OPLS-DA scatter plot (Figure 3A) showed that the exposed group could be clearly separated from the control group based on the 1400 peaks detected by UHPLC−(+)ESI−MS. The quality of the OPLS-DA model was first evaluated by $R^2(Y)$ and Q^2(cum) parameters, which indicate the fitness and prediction capability, respectively. Using one predictive and two orthogonal (1 + 2) components, the OPLS-DA model showed an $R^2(X)$ value of 15.3%, an $R^2(Y)$ value of 73.9%, and a Q^2(cum) value of 53.8%. Moreover, statistical validation of the corresponding PLS-DA model was performed to investigate the overfitting of data in the OPLS-DA model. Validation with a permutation number of 100 generated intercepts of R^2 = 0.403 and Q^2 = −0.304 (Supporting Information Figure S4A). The OPLS-DA model for the negative data was produced with an $R^2(X)$ value of 13.2%, an $R^2(Y)$ value of 73.4%, and a Q^2(cum) value of 44.3% across one predictive and two orthogonal components and validation intercepts of R^2 = 0.412 and Q^2 = −0.343 (Figure 3B and Supporting Information Figure S4B). These results indicate that the OPLS-DA models derived from the UHPLC−(±)ESI−MS data were statistically valid and acceptable. When the elderly smokers were included in the models, the fitness and predictive ability of corresponding OPLS-DA

DOI: 10.1021/acs.jproteome.5b00134
J. Proteome Res. 2015, 14, 2583−2593

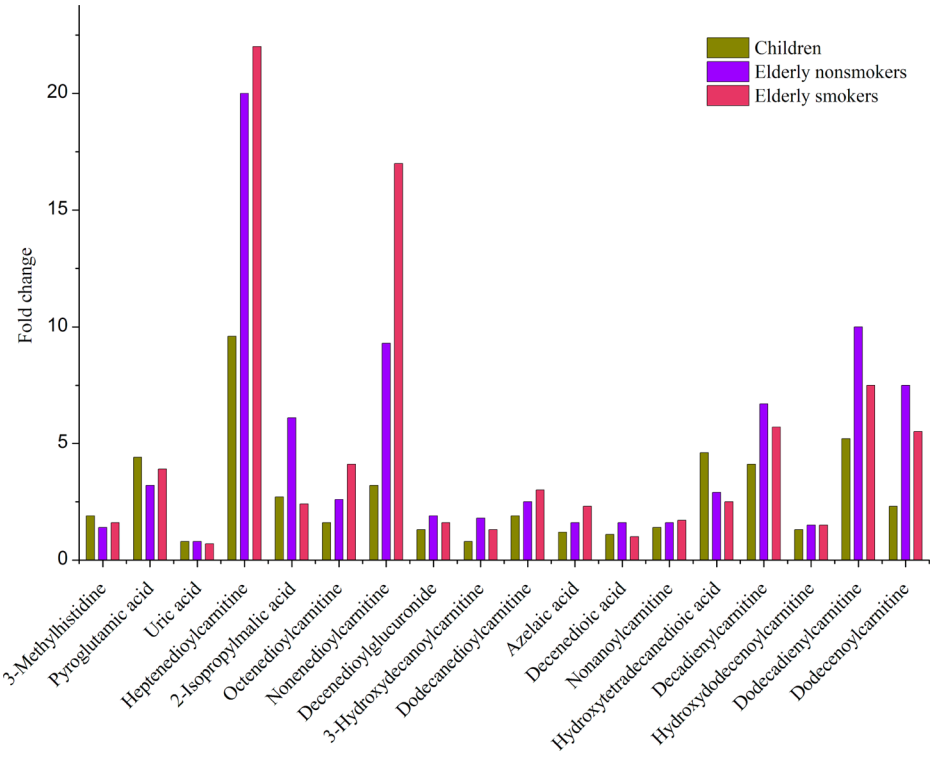

Figure 4. Fold change in the mean normalized peak areas of 18 discriminating metabolites between the exposed and control groups.

models using five latent variables were not as good, with $R^2(Y)$ = 71.7% and Q^2(cum) = 40.8% for UHPLC−(+)ESI−MS data and $R^2(Y)$ = 67.3% and Q^2(cum) = 29.5% for UHPLC−(−)ESI−MS data (Supporting Information Figure S5 and S6), which may be due to the confounding factor of smoking. To discover discriminating metabolites among the thousands of variables, the variable importance in the projection (VIP) value of each peak was calculated to indicate the contributions of the X variables to the OPLS-DA model. On the basis of the VIP threshold (VIP > 1.0) and $p < 0.05$ in Student's t test, 96 peaks that accounted for the class separation were selected as potential metabolic biomarkers of PAH exposure in elderly nonsmokers.

OPLS-DA was applied to the UHPLC−(±)ESI−MS data collected from children, which also showed a trend of separation between the control and exposed groups (Supporting Information Figure S7). Using three latent variables, the $R^2(X)$, $R^2(Y)$, and Q^2(cum) values were 13.2, 76.1, and 47.1%, respectively, for UHPLC−(+)ESI−MS data and 15.7, 60.0, and 32.1%, respectively, for UHPLC−(−)ESI−MS data. The intercepts of Q^2 for the corresponding PLS-DA models were less than 0.05, which indicated that the OPLS-DA models do not overfit (Supporting Information Figure S8). On the basis of the VIP threshold and p value, 84 peaks that accounted for the class separation were considered as potential metabolic biomarkers of PAH exposure in children.

The structures of the discriminating metabolites were identified based on our previously described strategy.[25,26] First, a molecular formula was determined according to the exact mass and the isotope pattern. Second, the elemental compositions were compared with those registered in the public databases METLIN (http://metlin.scripps.edu/), MassBank (http://www.massbank.jp/?lang=en), and HMDB (http://hmdb.ca/). Third, MS/MS experiments were conducted to obtain structural information based on the interpretation of the metabolites' fragmentation pattern. Finally, commercially available standards were adopted to confirm the structure of some metabolites, based on their retention time and product ion spectrum. As a result, a total of 18 discriminating metabolites were provisionally identified in elderly nonsmokers by this approach (Table 2). Five discriminating metabolites, including 3-methylhistidine, pyroglutamic acid, uric acid, 2-isopropylmalic acid, and azelaic acid, were further confirmed by comparison with authentic standards. Due to the lack of standards, the remaining 13 discriminating metabolites were tentatively identified based on their mass spectrometry data (Supporting Information Figures S9−S21). Ten discriminating metabolites that were tentatively identified in children were identical to those identified in elderly nonsmokers (Supporting Information Table S6). The peak areas and detection rates of these 18 metabolites are shown in Supporting Information Tables S7 and S8. The fold changes in the peak areas and the relative differences in detection rates of these 18 metabolites between the exposed and control groups are shown in Figure 4 and Supporting Information Figure S22.

Dose−Response Relationships between PAH Exposure and Metabolic Outcomes

Logistic regression analysis was performed to evaluate the association of PAH metabolites with the detection rates of the discriminating metabolites (Supporting Information Tables S9−S11). Among the elderly nonsmokers, the detection rates of pyroglutamic acid, 2-isopropylmalic acid, heptenedioylcarnitine, and dodecenoylcarnitine were significantly associated with one or more PAH metabolites including 1-OHN, 1-OHPH, 3-OHPH, 4-OHPH, 6-OHC, and ∑OH-PAHs ($p < 0.05$). Among the children, the detection rates of pyroglutamic acid, 2-isopropylmalic acid, decenedioic acid, dodecenoylcarnitine, heptenedioylcarnitine, hydroxytetradecanedioic acid, and non-

DOI: 10.1021/acs.jproteome.5b00134
J. Proteome Res. 2015, 14, 2583−2593

enedioylcarnitine were significantly associated with one or more PAH metabolites including 1-OHN, 2-OHF, 1-OHPH, 2-OHPH, 3-OHPH, 4-OHPH, and ∑OH-PAHs ($p < 0.05$). Among the elderly smokers, the detection rates of dodecenoylcarnitine, decadienylcarnitine, nonenedioylcarnitine, heptenedioylcarnitine, and dodecadienylcarnitine were significantly associated with one or more PAH metabolites including 2-OHF, 1-OHPH, 2-OHPH, 1-OHP, and ∑OH-PAHs ($p < 0.05$).

We further conducted one-dimensional linear regression models to estimate the association of the PAH metabolites with the discriminating metabolites in different populations (Supporting Information Tables S12−S14). The concentrations of the PAH metabolites and the peak areas of the discriminating metabolites were all log-transformed in the one-dimensional linear regression models. Among the elderly nonsmokers, 3-methylhistidine, dodecadienylcarnitine, nonanoylcarnitine, 3-hydroxydecanoylcarnitine, and hydroxydodecenoylcarnitine showed a significant dose−response relationship with one or more PAH metabolites including 1-OHPH, 2-OHPH, 3-OHPH, 1-OHP, and ∑OH-PAHs ($p < 0.05$). Each percentage point increase in ∑OH-PAHs results in a 0.42% increase in nonanoylcarnitine, a 0.39% increase in 3-methylhistidine, and a 0.36% increase in hydroxydodecenoylcarnitine ($p < 0.05$). Among the children, azelaic acid, dodecadienylcarnitine, and octenedioylcarnitine showed a significant dose−response he trelationship with one or more PAH metabolites including 1-OHN, 2-OHF, 1-OHPH, 2-OHPH, 3-OHPH, 4-OHPH, 1-OHP, 6-OHC, and ∑OH-PAHs ($p < 0.05$). Each percentage point increase in ∑OH-PAHs generates a 0.90% increase in dodecadienylcarnitine and a 0.22% increase in octenedioylcarnitine ($p < 0.05$). Among the elderly smokers, 3-methylhistidine, dodecadienylcarnitine, octenedioylcarnitine, nonanoylcarnitine, decenedioic acid, and 3-hydroxydecanoylcarnitine showed a significant dose−response relationship with one or more PAH metabolites including 2-OHN, 2-OHF, 1-OHPH, 2-OHPH, 3-OHPH, 1-OHP, and 1-OHC ($p < 0.05$).

DISCUSSION

We comprehensively evaluated the exposure of children and elderly adults to PAH pollutants by measuring nine urinary monohydroxylated metabolites of naphthalene, fluorene, phenanthrene, pyrene, and chrysene, which are representative of different PAH components. The urinary concentrations of most PAH metabolites were significantly higher in the exposed group than those in the control group, indicating that the participants from the polluted area were subjected to higher levels of PAH pollutants than those from the control area. The mean urinary 1-OHP concentration (1.96 μg/g creatinine for children, 1.42 μg/g creatinine for elderly nonsmokers, and 3.13 μg/g creatinine for elderly smokers) in the exposed population in the current study is comparable to that in children and adults living in a polluted area of Silesia, Poland (1.88 μg/g creatinine for children and 1.71−6.35 μg/g creatinine for adults),[27,28] lower than that in a Chinese general population living in a northern rural area of Jiangsu Province, China (6.35 μg/g creatinine for adults),[29] and higher than that in the American general population (0.164 μg/g creatinine for children and 0.122 μg/g creatinine for adults).[30] From these comparisons, we conclude the participants in the current study were exposed to moderate or relatively low levels of PAH pollutants.

The importance of biological monitoring for naphthalene, fluorene, and phenanthrene has been highlighted by several studies that confirmed the toxicities of these molecules and their presence in living environments.[22,31,32] In this study, the urinary levels of 1-OHN, 2-OHN, 2-OHF, 1-OHPH, and 3-OHPH were higher than that of 1-OHP. For elderly nonsmokers and children, the differences in the levels of urinary 1-OHN and 1-OHPH between the exposed and control groups were greater than the difference in the 1-OHP urinary concentration. Moreover, 1-OHPH showed a closer association with ∑OH-PAHs ($r = 0.73$ in elderly nonsmokers and 0.64 in children) than 1-OHP ($r = 0.53$ in elderly nonsmokers and 0.49 in children). Moreover, the association of 1-OHPH with the metabolic outcomes was roughly equivalent to that of 1-OHP. For elderly smokers, the difference in the urinary concentration of 1-OHP between the exposed and control groups was roughly equivalent to the difference in the 1-OHPH urinary concentration, and 1-OHP showed approximately the same association with ∑OH-PAHs as that of 1-OHPH. However, 1-OHP showed a closer association with the metabolic outcomes than 1-OHP. On the basis of these facts, we conclude that 1-OHPH may be a more sensitive and reliable biomarker than 1-OHP to evaluate total environmental PAH exposure and its metabolic outcomes in nonoccupationally exposed populations.

Previous studies indicate that oxidative stress may play a key role in the etiology of various PAH-related diseases, such as cardiovascular diseases, chronic pulmonary diseases, and cancers.[33−35] However, the early molecular events in the exposure−disease continuum are not yet fully understood. Identifying multiple intermediate biomarkers, which can serve as combinatorial signatures of the early molecular events of toxicity, will provide complementary information to the exposure assessment and is crucial to allow accurate early health risk assessment.[14] Metabolomics, which can characterize the interactions among lifestyle, the environment, and the genes that determine diseases,[36] is a powerful tool for identifying of new intermediate biomarkers and can be used as an information-rich end point in molecular epidemiology.[14] Here, we systematically investigated the urinary metabolic changes in humans with chronic environmental PAHs exposure using a sensitive UHPLC−MS-based global metabolomic approach. As a result, 18 significantly changed urinary metabolites were identified in individuals exposed to coking industry-related pollutions. Most of the metabolites, including two amino acids (3-methylhistidine and pyroglutamic acid), three organic acids (2-isopropylmalic acid, azelaic acid, decenedioic acid, and hydroxytetradecanedioic acid), one glucuronide conjugate (decenedioylglucuronide), and 11 acylcarnitines (heptenedioylcarnitine, octenedioylcarnitine, nonenedioylcarnitine, 3-hydroxydecanoylcarnitine, dodecanedioylcarnitine, nonanoylcarnitine, decadienylcarnitine, hydroxydodecenoylcarnitine, dodecadienylcarnitine, and dodecenoylcarnitine) were significantly increased in the exposed populations. Uric acid was the only metabolite that was significantly decreased in the exposed populations.

The concentration of pyroglutamic acid was significantly increased in the exposed populations. Pyroglutamic acid is an intermediate metabolite of the γ-glutamyl cycle through which glutathione is synthesized and degraded.[37] Urinary pyroglutamic acid has been identified as potential biomarker of oxidative stress induced by chronic cadmium exposure in humans.[16] The concentration of uric acid was significantly decreased in the exposed children and elderly nonsmokers. Uric acid is a

DOI: 10.1021/acs.jproteome.5b00134
J. Proteome Res. 2015, 14, 2583−2593

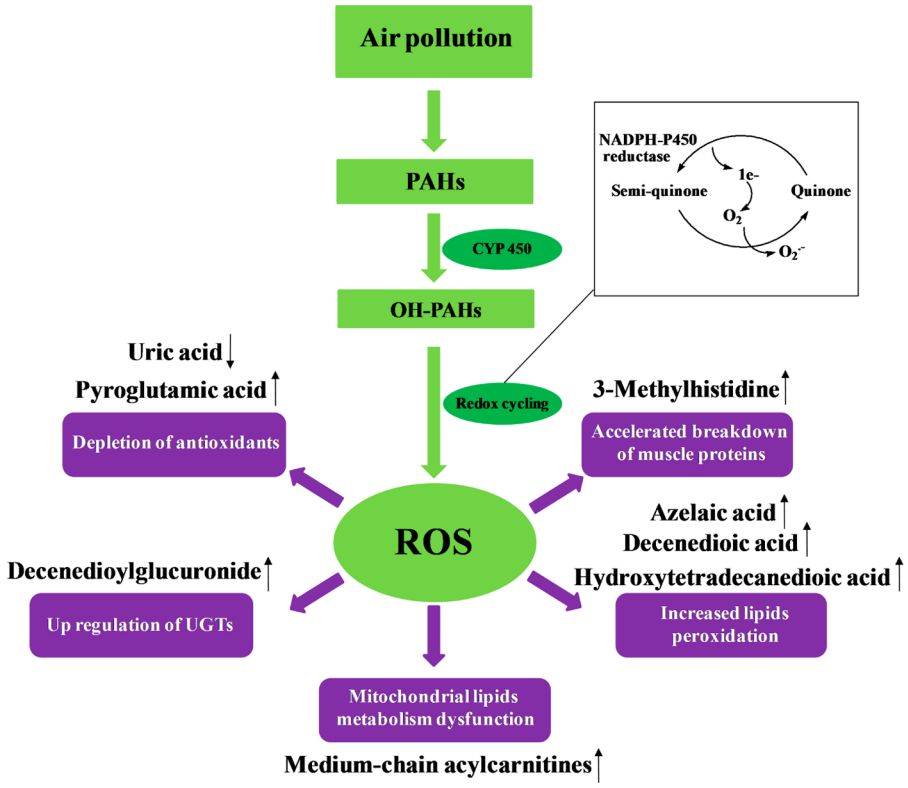

Figure 5. Proposed relationship between PAH exposure and metabolic outcomes. ROS, reactive oxygen species; UGTs, UDP-glucuronosyltransferases.

powerful antioxidant and end product of purine metabolism. The reaction of uric acid with superoxides and hydroxyl radicals results in the scavenging of reactive oxygen species (ROS) and the formation of allantoin. When both elevated pyroglutamic acid levels and decreased uric acid levels are considered together, we speculate that the higher PAH burden in the exposed populations may result in excessive ROS production, promoting the depletion of the antioxidant glutathione and uric acid.

We observed a significant increase in the urinary 3-methylhistidine level in the exposed populations. 3-Methylhistidine is an important constituent of muscle proteins, and urinary 3-methylhistidine has been used to estimate the rate of muscle protein breakdown.[38] Oxidative stress can reportedly promote muscle protein breakdown in three major ways: (1) increasing the gene expression of key proteins involved in autophagy, calpain, and the proteasome system of proteolysis; (2) activating calpain and caspase-3; and (3) modifying the structures of myofibrillar proteins and enhancing their susceptibility to proteolytic processing.[39] The elevated level of 3-methylhistidine in the exposed population suggests that the higher PAHs burden in the body causes increased oxidative stress, thus promoting the breakdown of muscle protein and the release of 3-methylhistidine.

The levels of several unusual medium-chain (6−12 carbons) acylcarnitines were significantly increased in the exposed populations. Medium-chain acylcarnitines are synthesized with L-carnitine and the corresponding medium-chain fatty acids,[40] which primarily originate from incomplete mitochondrial β-oxidation of long-chain fatty acids and/or lipid peroxidation.[41] The conjugation of organic acids with L-carnitine could facilitate their urinary excretion, protecting cells from the detrimental effects of the organic acids' accumulation in the body.[42] The levels of azelaic acid, decenedioic acid, and hydroxytetradecanedioic acid, which are byproducts of lipid peroxidation and indicators of oxidative stress, were also significantly elevated in the exposed elders.[43] The increased levels of unusual medium-chain acylcarnitines and organic acids in this study may be related to increased lipid peroxidation or the dysfunction of the mitochondrial oxidative lipid metabolism in the exposed populations.

The concentration of decenedioylglucuronide was significantly elevated in the elderly nonsmokers. Formation of decenedioylglucuronide is catalyzed by UDP-glucuronosyltransferases (UGTs), which catalyze the conjugation of xenobiotics or their reactive metabolites with glucuronic acid and, thus, act as indirect antioxidants.[44] The expression of UGTs can be induced by oxidative stress and xenobiotic exposure (e.g., PAHs).[44] Although acyl glucuronides are suspected to have an association with the cytotoxic, carcinogenic, and idiosyncratic immunologic toxicities of some carboxylic acid drugs,[45−47] glucuronidation is generally believed to play an important role in the detoxification of xenobiotics because glucuronides usually have less intrinsic biological or chemical activity than their parental aglycones and are rapidly excreted.[44,48] The increased levels of decenedioylglucuronide may be associated with the upregulation of UGTs in the exposed elderly nonsmokers. The urinary 2-isopropylmalic acid concentration was significantly elevated in the exposed elderly nonsmokers. It may be associated with the alterations in leucine metabolism, but the underlying mechanisms remained unclear.

To summarize, the metabolic outcomes of PAH exposure were generally associated with oxidative stress. One possible explanation for these results is that increased levels of PAHs in the body may induce the expression of phase I and phase II

DOI: 10.1021/acs.jproteome.5b00134
J. Proteome Res. 2015, 14, 2583−2593

enzymes. This would trigger the metabolic activation of PAHs, resulting in the generation of semiquinone radicals and ROS and thereby causing the depletion of antioxidants, lipid peroxidation, dysfunction of the mitochondrial lipid metabolism, accelerated breakdown of muscle proteins, and upregulation of UGTs.[49,50] The proposed relationship between PAH exposure and its metabolic outcomes are summarized in Figure 5.

Although levels of PAH exposure were relatively low in the present study, a number of discriminating metabolites were found to have a significant linear dose−response relationship with PAH exposure. Among these metabolites, dodecadienylcarnitine was the most important metabolite for discriminating between the exposed and control groups among elderly nonsmokers and children, with a VIP value of 13 for the elderly nonsmokers groups and a VIP value of 8.4 for the children's groups. The urinary concentration of dodecadienylcarnitine in the elderly nonsmokers, children, and elderly smokers was 10, 5.2, and 7.5 times higher in the exposed group than that in the control group, respectively. Moreover, dodecadienylcarnitine showed a dose-dependent association with multiple PAH metabolites among all three populations, and dodecadienylcarnitine was the only metabolite that showed a significant linear dose−response relationship with 1-OHPH among all three populations. On the basis of these facts, we tentatively proposed that urinary dodecadienylcarnitine may be developed as a novel and sensitive biomarker for monitoring PAH-induced oxidative stress in the nonoccupationally exposed population. Furthermore, the linear regression coefficient between dodecadienylcarnitine and 1-OHPH was much higher in elderly smokers (β = 2.09) than that in elderly nonsmokers (β = 0.78) and children (β = 0.73), suggesting that elderly smokers may be more sensitive to PAH-induced oxidative damage than elderly nonsmokers and children.

The present study has strengths and limitations. First, this is the first study to investigate the human metabolic responses to chronic environmental PAH exposure in a large susceptible Chinese population, including children and elders. Second, because the absorption of PAHs in the same environment may vary among individuals, the 9 urinary PAH metabolites measured in this study allow the PAH exposure level of each individual to be comprehensively evaluated. However, other redox-active toxicants, such as ozone, metals, and nitrogen dioxide, are also present in the emissions from the coking industry, which may also contribute to oxidative stress-related responses in the body[51,52] and need to be evaluated in future studies.

CONCLUSIONS

Using a LC−MS-based metabolomic approach, we investigated, for the first time, the urinary metabolic changes in humans with different levels of PAH exposure. As a result, 18 discriminating metabolites related to amino acid, purine, and lipid metabolism significantly varied between individuals in the exposed and control groups. These findings suggest that chronic environmental exposure to low levels of PAHs has oxidative stress-related effects in humans. Moreover, 1-OHPH and dodecadienylcarnitine are potential sensitive and reliable biomarkers for monitoring PAH exposure and its metabolic outcomes in the general population, respectively. This study demonstrates that a metabolomic approach is a useful tool to identify the various metabolic changes of environmental PAH exposure in the general population and provides new insight into the mechanisms underlying PAH-induced toxic effects. The study also indicates that dietary or supplemental intake of antioxidants that can neutralize ROS and reverse oxidative stress in the body may be useful to reduce the PAH exposure-induced detrimental effects and prevent the etiology of various PAH-related diseases.

ASSOCIATED CONTENT

Supporting Information

The program used for peak discrimination, filtering, alignment and CAMERA analysis in the UHPLC−(+)ESI−MS and UHPLC−(−)ESI−MS data. Table S1: LC parameters for the analysis of urinary PAH metabolites. Table S2: MS parameters for the analysis of urinary PAH metabolites. Table S3: Levels of urinary PAH metabolites in the control and exposed groups. Table S4: Levels of urinary PAH metabolites in elderly male nonsmokers and smokers. Table S5: Pearson correlation coefficients between PAH metabolites in the exposed group. Table S6: Tentatively identified metabolites capable of discriminating between children in the exposed and control groups. Table S7: Normalized peak areas of 18 discriminating metabolites in the control and exposed groups. Table S8: Detection rates of 18 discriminating metabolites in the control and exposed groups. Table S9: Results for the logistic regression of PAH exposure and the metabolic outcomes in elderly nonsmokers. Table S10: Results for the logistic regression of PAH exposure and the metabolic outcomes in children. Table S11: Results for the logistic regression of PAH metabolites and the metabolic outcomes in elderly smokers. Table S12: Results for the linear regression of PAH exposure and the metabolic outcomes in elderly nonsmokers. Table S13: Results for the linear regression of PAH exposure and the metabolic outcomes in children. Table S14: Results for the linear regression of PAH exposure with the metabolic outcomes in elderly smokers. Figure S1: Typical TICs obtained from the urine samples of the different groups by UHPLC−(+)ESI−MS. Figure S2: Line plots of quality control (QC) samples generated by PCA using components 1 and 2. Figure S3: Retention time deviation profiles derived from UHPLC−(+)ESI−MS and UHPLC−(−)ESI−MS analyses. Figure S4: PLS-DA validation plots of 100 random permutations based on the UHPLC−(+)ESI−MS and UHPLC−(−)ESI−MS data from elderly nonsmokers. Figure S5: OPLS-DA score plots based on the UHPLC−(+)ESI−MS and UHPLC−(−)ESI−MS data from elderly adults (including smokers and nonsmokers). Figure S6: PLS-DA validation plots of 100 random permutations based on the UHPLC−(+)ESI−MS and UHPLC−(−)ESI−MS data from elderly adults (including smokers and nonsmokers). Figure S7: OPLS-DA score plots based on the UHPLC−(+)ESI−MS and UHPLC−(−)ESI−MS data from children. Figure S8: PLS-DA validation plots of 100 random permutations based on the UHPLC−(+)ESI−MS and UHPLC−(−)ESI−MS data from children. Figure S9: MS data used for identification of heptenedioylcarnitine. Figure S10: MS data used for identification of octenedioylcarnitine. Figure S11: MS data used for identification of nonenedioylcarnitine. Figure S12: MS data used for identification of decenedioylglucuronide. Figure S13: MS data used for identification of 3-hydroxydecanoylcarnitine. Figure S14: MS data used for identification of dodecanedioylcarnitine. Figure S15: MS data used for identification of decenedioic acid. Figure S16: MS data used for identification of nonanoylcarnitine.

DOI: 10.1021/acs.jproteome.5b00134
J. Proteome Res. 2015, 14, 2583−2593

Figure S17: MS data used for identification of hydroxytetradecanedioic acid. Figure S18: MS data used for identification of decadienylcarnitine. Figure S19: MS data used for identification of hydroxydodecenoylcarnitine. Figure S20: MS data used for identification of dodecadienylcarnitine. Figure S21: MS data used for identification of dodecenoylcarnitine. Figure S22: The relative difference in the detection rate of 18 discriminating metabolites between the exposed and control groups. The Supporting Information is available free of charge on the ACS Publications website at DOI: 10.1021/acs.jproteome.5b00134.

AUTHOR INFORMATION

Corresponding Authors

*(R.Z.) Tel.: +86 10-63165310; Fax: +86 10-63153121; E-mail: rpzhang@imm.ac.cn.
*(Z.A.) Tel.: +86 10-63165218; Fax: +86 10-63165218; E-mail: zeper@imm.ac.cn.

Notes

The authors declare no competing financial interest.

ACKNOWLEDGMENTS

This research was supported by the National High Technology Research and Development Program of China (863 Program) (no. 2014AA021101).

REFERENCES

(1) Mastrangelo, G.; Fadda, E.; Marzia, V. Polycyclic aromatic hydrocarbons and cancer in man. *Environ. Health Perspect.* **1996**, *104*, 1166.
(2) Burstyn, I.; Boffetta, P.; Heederik, D.; Partanen, T.; Kromhout, H.; Svane, O.; Langård, S.; Frentzel-Beyme, R.; Kauppinen, T.; Stücker, I.; Shaham, J.; Ahrens, W.; Cenée, S.; Ferro, G.; Heikkilä, P.; Hooiveld, M.; Johansen, C.; Randem, B. G.; Schill, W. Mortality from obstructive lung diseases and exposure to polycyclic aromatic hydrocarbons among asphalt workers. *Am. J. Epidemiol.* **2003**, *158*, 468−478.
(3) Armstrong, B. G.; Gibbs, G. Exposure−response relationship between lung cancer and polycyclic aromatic hydrocarbons (PAHs). *Occup. Environ. Med.* **2009**, *66*, 740−746.
(4) Gatto, M. P.; Gariazzo, C.; Gordiani, A.; L'Episcopo, N.; Gherardi, M. Children and elders exposure assessment to particle-bound polycyclic aromatic hydrocarbons (PAHs) in the city of Rome, Italy. *Environ. Sci. Pollut. Res. Int.* **2003**, 1−8.
(5) Hubal, E. C.; Sheldon, L. S.; Burke, J. M.; McCurdy, T. R.; Berry, M. R.; Rigas, M. L.; Zartarian, V. G.; Freeman, N. C. Children's exposure assessment: a review of factors influencing children's exposure, and the data available to characterize and assess that exposure. *Environ. Health Perspect.* **2000**, *108*, 475−486.
(6) Adler, T. Aging research: the future face of environmental health. *Environ. Health Perspect.* **2003**, *111*, A760.
(7) Makri, A.; Stilianakis, N. I. Vulnerability to air pollution health effects. *Int. J. Hyg. Environ. Health* **2008**, *211*, 326−336.
(8) Stokstad, E. Biomonitoring: pollution gets personal. *Science* **2004**, *304*, 1892−1894.
(9) Scherer, G.; Frank, S.; Riedel, K.; Meger-Kossien, I.; Renner, T. Biomonitoring of exposure to polycyclic aromatic hydrocarbons of nonoccupationally exposed persons. *Cancer Epidemiol., Biomarkers Prev.* **2000**, *9*, 373−380.
(10) Jacob, J.; Seidel, A. Biomonitoring of polycyclic aromatic hydrocarbons in human urine. *J. Chromatogr. B: Anal. Technol. Biomed. Life Sci.* **2002**, *778*, 31−47.
(11) Serdar, B.; Waidyanatha, S.; Zheng, Y.; Rappaport, S. M. Simultaneous determination of urinary 1- and 2-naphthols, 3- and 9-phenanthrols, and 1-pyrenol in coke oven workers. *Biomarkers* **2003**, *8*, 93−109.
(12) Vineis, P.; Perera, F. Molecular epidemiology and biomarkers in etiologic cancer research: the new in light of the old. *Cancer Epidemiol., Biomarkers Prev.* **2007**, *16*, 1954−1965.
(13) Chadeau-Hyam, M.; Athersuch, T. J.; Keun, H. C.; De, I. M.; Ebbels, T. M.; Jenab, M.; Sacerdote, C.; Bruce, S. J.; Holmes, E.; Vineis, P. Meeting-in-the-middle using metabolic profiling—a strategy for the identification of intermediate biomarkers in cohort studies. *Biomarkers* **2011**, *16*, 83−88.
(14) Ellis, J. K.; Athersuch, T. J.; Thomas, L. D.; Teichert, F.; Pérez-Trujillo, M.; Svendsen, C.; Spurgeon, D. J.; Singh, R.; Järup, L.; Bundy, J. G.; Keun, H. C. Metabolic profiling detects early effects of environmental and lifestyle exposure to cadmium in a human population. *BMC Med.* **2012**, *10*, 61.
(15) Vulimiri, S. V.; Berger, A.; Sonawane, B. The potential of metabolomic approaches for investigating mode(s) of action of xenobiotics: case study with carbon tetrachloride. *Mutat. Res.* **2011**, *722*, 147−153.
(16) Gao, Y.; Lu, Y.; Huang, S.; Gao, L.; Liang, X.; Wu, Y.; Wang, J.; Huang, Q.; Tang, L.; Wang, G.; Yang, F.; Hu, S.; Chen, Z.; Wang, P.; Jiang, Q.; Huang, R.; Xu, Y.; Yang, X.; Ong, C. N. Identifying early urinary metabolic changes with long-term environmental exposure to cadmium by mass spectrometry-based metabolomics. *Environ. Sci. Technol.* **2014**, *48*, 6409−6418.
(17) Shen, H.; Xu, W.; Zhang, J.; Chen, M.; Martin, F. L.; Xia, Y.; Liu, L.; Zhu, Y. G. Urinary metabolic biomarkers link oxidative stress indicators associated with general arsenic exposure to male infertility in a Han Chinese population. *Environ. Sci. Technol.* **2013**, *47*, 8843−8851.
(18) Kuo, C. H.; Wang, K. C.; Tian, T. F.; Tsai, M. H.; Chiung, Y. M.; Hsiech, C. M.; Tsai, S. J.; Wang, S. Y.; Tsai, D. M.; Huang, C. C.; Tseng, Y. J. Metabolomic characterization of laborers exposed to welding fumes. *Chem. Res. Toxicol.* **2012**, *25*, 676−686.
(19) Xu, X.; Zhang, J.; Zhang, L.; Liu, W.; Weisel, C. P. Selective detection of monohydroxy metabolites of polycyclic aromatic hydrocarbons in urine using liquid chromatography/triple quadrupole tandem mass spectrometry. *Rapid Commun. Mass Spectrom.* **2004**, *18*, 2299−2308.
(20) Gika, H. G.; Theodoridis, G. A.; Wingate, J. E.; Wilson, I. D. Within-day reproducibility of an HPLC-MS-based method for metabonomic analysis: application to human urine. *J. Proteome Res.* **2007**, *6*, 3291−3303.
(21) Yang, M.; Koga, M.; Katoh, T.; Kawamoto, T. A study for the proper application of urinary naphthols, new biomarkers for airborne polycyclic aromatic hydrocarbons. *Arch. Environ. Contam. Toxicol.* **1999**, *36*, 99−108.
(22) Toriba, A.; Chetiyanukornkul, T.; Kizu, R.; Hayakawa, K. Quantification of 2-hydroxyfluorene in human urine by column-switching high performance liquid chromatography with fluorescence detection. *Analyst* **2009**, *128*, 605−610.
(23) Boogaard, P. J.; Van Sittert, N. J. Biological monitoring of exposure to benzene: a comparison between S-phenylmercapturic acid, *trans,trans*-muconic acid, and phenol. *Occup. Environ. Med.* **1995**, *52*, 611−620.
(24) Wagner, S.; Scholz, K.; Donegan, M.; Burton, L.; Wingate, J.; Völkel, W. Metabonomics and biomarker discovery: LC−MS metabolic profiling and constant neutral loss scanning combined with multivariate data analysis for mercapturic acid analysis. *Anal. Chem.* **2006**, *78*, 1296−1305.
(25) Xu, J.; Chen, Y.; Zhang, R.; Song, Y.; Cao, J.; Bi, N.; Wang, J.; He, J.; Bai, J.; Dong, L.; Wang, L.; Zhan, Q.; Abliz, Z. Global and targeted metabolomics of esophageal squamous cell carcinoma discovers potential diagnostic and therapeutic biomarkers. *Mol. Cell. Proteomics* **2013**, *12*, 1306−1318.
(26) An, Z.; Chen, Y.; Zhang, R.; Song, Y.; Sun, J.; He, J.; Bai, J.; Dong, L.; Zhan, Q.; Abliz, Z. Integrated ionization approach for RRLCMS/MS-based metabonomics: finding potential biomarkers for lung cancer. *J. Proteome Res.* **2010**, *9*, 4071−4081.

DOI: 10.1021/acs.jproteome.5b00134
J. Proteome Res. 2015, 14, 2583−2593

(27) Siwińska, E.; Mielżyńska, D.; Bubak, A.; Smolik, E. The effect of coal stoves and environmental tobacco smoke on the level of urinary 1-hydroxypyrene. *Mutat. Res.* **1999**, *445*, 147−153.
(28) Ovrebø, S.; Fjeldstad, P. E.; Grzybowska, E.; Kure, E. H.; Chorazy, M.; Haugen, A. Biological monitoring of polycyclic aromatic hydrocarbon exposure in a highly polluted area of Poland. *Environ. Health Perspect.* **1995**, *103*, 838−843.
(29) Yin, W. Q.; Wang, L.; Li, R. R.; Cao, S. Y.; Ye, Y. T.; Li, L. Personal exposure levels of PAHs in the general population in northern rural area of Jiangsu Province, China. *J. Environ. Sci. Health, Part A: Toxic/Hazard. Subst. Environ. Eng.* **2014**, *49*, 281−286.
(30) *Fourth National Report on Human Exposure to Environmental Chemicals*; Centers for Disease Control and Prevention: Atlanta, GA, 2009. http://www.cdc.gov/exposurereport/pdf/fourthreport.pdf.
(31) Preuss, R.; Angerer, J.; Drexler, H. Naphthalene—an environmental and occupational toxicant. *Int. Arch. Occup. Environ. Health* **2003**, *76*, 556−576.
(32) Elovaara, E.; Väänänen, V.; Mikkola, J. Simultaneous analysis of naphthols, phenanthrols, and 1-hydroxypyrene in urine as biomarkers of polycyclic aromatic hydrocarbon exposure: intraindividual variance in the urinary metabolite excretion profiles caused by intervention with β-naphthoflavone induction in the rat. *Arch. Toxicol.* **2003**, *77*, 183−193.
(33) Mena, S.; Ortega, A.; Estrela, J. M. Oxidative stress in environmental-induced carcinogenesis. *Mutat. Res.* **2009**, *674*, 36−44.
(34) Gross, M.; Steffes, M.; Jacobs, D. R., Jr.; Yu, X.; Lewis, L.; Lewis, C. E.; Loria, C. M. Plasma F2-isoprostanes and coronary artery calcification: The CARDIA Study. *Clin. Chem.* **2005**, *51*, 125−131.
(35) Chung, K. F.; Marwick, J. A. Molecular mechanisms of oxidative stress in airways and lungs with reference to asthma and chronic obstructive pulmonary disease. *Ann. N.Y. Acad. Sci.* **2010**, *1203*, 85−91.
(36) Holmes, E.; Loo, R. L.; Stamler, J.; Bictash, M.; Yap, I. K.; Chan, Q.; Ebbels, T.; De, I. M.; Brown, I. J.; Veselkov, K. A.; Daviglus, M. L.; Kesteloot, H.; Ueshima, H.; Zhao, L.; Nicholson, J. K.; Elliott, P. Human metabolic phenotype diversity and its association with diet and blood pressure. *Nature* **2008**, *453*, 396−400.
(37) Pederzolli, C. D.; Sgaravatti, Â. M.; Braum, C. A.; Prestes, C. C.; Zorzi, G. K.; Sgarbi, M. B.; Wyse, A. T.; Wannmacher, C. M.; Wajner, M.; Dutra-Filho, C. S. 5-Oxoproline reduces non-enzymatic antioxidant defenses in vitro in rat brain. *Metab. Brain Dis.* **2007**, *22*, 51−65.
(38) Rennie, M. J.; Phillips, S.; Smith, K. Reliability of results and interpretation of measures of 3-methylhistidine in muscle interstitium as marker of muscle proteolysis. *J. Appl. Physiol.* **2008**, *105*, 1380−1381.
(39) Powers, S. K.; Smuder, A. J.; Criswell, D. S. Mechanistic links between oxidative stress and disuse muscle atrophy. *Antioxid. Redox Signaling* **2011**, *15*, 2519−2528.
(40) Mentlein, R.; Reuter, G.; Heymann, E. Specificity of two different purified acylcarnitine hydrolases from rat liver, their identity with other carboxylesterases, and their possible function. *Arch. Biochem. Biophys.* **1985**, *240*, 801−810.
(41) Chen, J.; Wang, W.; Lv, S.; Yin, P.; Zhao, X.; Lu, X.; Zhang, F.; Xu, G. Metabonomics study of liver cancer based on ultra performance liquid chromatography coupled to mass spectrometry with HILIC and RPLC separations. *Anal. Chim. Acta* **2009**, *650*, 3−9.
(42) Chapela, S. P.; Kriguer, N.; Fernández, E. H.; Stella, C. A. Involvement of L-carnitine in cellular metabolism: beyond Acyl-CoA transport. *Mini-Rev. Med. Chem.* **2009**, *9*, 1518−1526.
(43) Maes, M.; Mihaylova, I.; Leunis, J. C. Chronic fatigue syndrome is accompanied by an IgM-related immune response directed against neopitopes formed by oxidative or nitrosative damage to lipids and proteins. *Neuroendocrinol. Lett.* **2006**, *27*, 615−621.
(44) Kalthoff, S.; Ehmer, U.; Freiberg, N.; Manns, M. P.; Strassburg, C. P. Interaction between oxidative stress sensor Nrf2 and xenobiotic-activated aryl hydrocarbon receptor in the regulation of the human phase II detoxifying UDP-glucuronosyltransferase 1A10. *J. Biol. Chem.* **2010**, *285*, 5993−6002.
(45) Ritter, J. K. Roles of glucuronidation and UDP-glucuronosyltransferases in xenobiotic bioactivation reactions. *Chem.−Biol. Interact.* **2000**, *129*, 171−193.
(46) Sallustio, B. C.; DeGraaf, Y. C.; Weekley, J. S.; Burcham, P. C. Bioactivation of carboxylic acid compounds by UDP-glucuronosyltransferases to DNA-damaging intermediates: role of glycoxidation and oxidative stress in genotoxicity. *Chem. Res. Toxicol.* **2006**, *19*, 683−691.
(47) Nicholls, A. W.; Akira, K.; Lindon, J. C.; Farrant, R. D.; Wilson, I. D.; Harding, J.; Killick, D. A.; Nicholson, J. K. NMR spectroscopic and theoretical chemistry studies on the internal acyl migration reactions of the 1-*O*-acyl-β-D-glucopyranuronate conjugates of 2-, 3-, and 4-(trifluoromethyl) benzoic acids. *Chem. Res. Toxicol.* **1996**, *9*, 1414−1424.
(48) Rowland, A.; Miners, J. O.; Mackenzie, P. I. The UDP-glucuronosyltransferases: their role in drug metabolism and detoxification. *Int. J. Biochem. Cell Biol.* **2013**, *45*, 1121−1132.
(49) Penning, T. M.; Drury, J. E. Human aldo-keto reductases: function, gene regulation, and single nucleotide polymorphisms. *Arch. Biochem. Biophys.* **2007**, *464*, 241−250.
(50) Palackal, N. T.; Lee, S. H.; Harvey, R. G.; Blair, I. A.; Penning, T. M. Activation of polycyclic aromatic hydrocarbon trans-dihydrodiol proximate carcinogens by human aldo-keto reductase (AKR1C) enzymes and their functional overexpression in human lung carcinoma (A549) cells. *J. Biol. Chem.* **2002**, *277*, 24799−24808.
(51) Chen, C.; Arjomandi, M.; Balmes, J.; Tager, I.; Holland, N. Effects of chronic and acute ozone exposure on lipid peroxidation and antioxidant capacity in healthy young adults. *Environ. Health Perspect.* **2007**, *115*, 1732−1737.
(52) Bae, S.; Pan, X. C.; Kim, S. Y.; Park, K.; Kim, Y. H.; Kim, H.; Hong, Y. C. Exposures to particulate matter and polycyclic aromatic hydrocarbons and oxidative stress in schoolchildren. *Environ. Health Perspect.* **2010**, *118*, 579−583.

DOI: 10.1021/acs.jproteome.5b00134
J. Proteome Res. 2015, 14, 2583−2593